Energetics of the Induced Structural Change in a Ca^{2+} Regulatory Protein: Ca^{2+} and Troponin I Peptide Binding to the E41A Mutant of the N-Domain of Skeletal Troponin C†

Ryan T. McKay, Linda F. Saltibus, Monica X. Li, and Brian D. Sykes*

CIHR Group in Protein Structure and Function, Department of Biochemistry, University of Alberta, 474 Medical Science Building, Edmonton, Alberta, Canada T6G 2H7

Received May 31, 2000; Revised Manuscript Received August 1, 2000

ABSTRACT: Structural studies have shown that the regulatory domains of skeletal and cardiac troponin C (sNTnC and cNTnC) undergo different conformational changes upon Ca^{2+} binding; sNTnC "opens" with a large exposure of the hydrophobic surface, while cNTnC retains a "closed" conformation similar to that in the apo state. This is mainly due to the fact that there is a defunct Ca^{2+}-binding site I in cNTnC. Despite the striking difference, the two proteins bind their respective troponin I (TnI) regions ($sTnI_{115-131}$ and $cTnI_{147-163}$, respectively) in a similar open fashion. Thus, there must exist a delicate energetic balance between Ca^{2+} and TnI binding and the accompanying conformational changes in TnC for each system. To understand the coupling between Ca^{2+} and TnI binding and the concomitant structural changes, we have previously engineered an E41A mutant of sNTnC and demonstrated that this mutation drastically reduced the Ca^{2+}-binding affinity of site I in sNTnC, and as a result, E41A-sNTnC remains closed in the Ca^{2+}-bound state. In the present work, we investigated the interaction of E41A-sNTnC with the $sTnI_{115-131}$ peptide and found that the peptide binds to the Ca^{2+}-saturated E41A-sNTnC with a 1:1 stoichiometry and a dissociation constant of 300 ± 100 μM. The peptide-induced chemical shift changes resemble those of Ca^{2+} binding to sNTnC, suggesting that $sTnI_{115-131}$ induces the "opening" of E41A-sNTnC. In addition, the binding of $sTnI_{115-131}$ appears to be accompanied by a conformational change in site I of E41A-sNTnC so that the damaged regulatory site can bind Ca^{2+} more tightly. Without Ca^{2+}, $sTnI_{115-131}$ only interacts with E41A-sNTnC nonspecifically. When Ca^{2+} is titrated into E41A-sNTnC in the presence of $sTnI_{115-131}$, the Ca^{2+}-binding affinity of site I was enhanced by ∼5-fold as compared to when $sTnI_{115-131}$ was not present. These observations suggest that the binding of Ca^{2+} and TnI is intimately coupled to each other. Together with our previous studies on Ca^{2+} and TnI peptide binding to sNTnC and cNTnC, these results allow us to dissect the mechanism and energetics of coupling of ligand binding and structural opening intricately involved in the regulation of skeletal and cardiac muscle contraction.

Calcium is an integral component of many proteins and serves both structural and regulatory functions (for a recent review, see ref *1*). The release of calcium ions in the muscle cell is a key event in the contractile signal pathway necessary for actomyosin−ATPase activity and muscle contraction. The calcium transient is recognized in muscle cells by the muscle regulatory protein troponin C. It is believed that Ca^{2+} binding to TnC initiates a cascade of structural changes in the muscle thin filament, which in turn modifies the interaction between the thick and thin filaments, leading to muscle contraction (for recent reviews, see refs *2*−*4*).

Two isoforms of TnC exist in striated muscle, fast skeletal muscle TnC (sTnC)[1] and slow skeletal/cardiac muscle TnC (cTnC). Both molecules are dumbbell-shaped with the N- and C-domains connected by a flexible linker in solution and comprise four EF-hand helix−loop−helix motifs as potential Ca^{2+}-binding sites (*5*, *6*). Sites I and II are paired as a unit in the N-domain, and sites III and IV form another pair in the C-domain. It is generally believed that the N-domain plays a regulatory role, while the C-domain is the structural counterpart. Ca^{2+} binding to TnC is coupled by induced structural changes in the N-domain. Structural studies have shown that sTnC undergoes a large Ca^{2+}-induced structural "opening" (*7*), while Ca^{2+} binding to cardiac muscle TnC results in minimal conformational

† This work was supported by the Canadian Institute of Health Research. R.T.M. was supported by an Alberta Heritage Foundation for Medical Research Studentship.

* Author to whom correspondence should be addressed. Phone: (403) 492-5460. Fax: (403) 492-0886. E-mail: brian.sykes@ualberta.ca.

[1] Abbreviations: sTnC, skeletal troponin C; cTnC, cardiac troponin C; sTnI, skeletal troponin I; sNTnC, N-domain of skeletal troponin C corresponding to residues 1−90; cNTnC, N-domain of cardiac troponin C corresponding to residues 1−89; E41A-sNTnC, E41A mutant of the N-domain of skeletal troponin C corresponding to residues 1−90; $sTnI_{115-131}$, synthetic skeletal troponin I peptide containing residues 115−131; $cTnI_{147-163}$, synthetic cardiac troponin I peptide containing residues 147−163; $\Delta\delta_i$, change $[(\Delta\delta^2_{1H} + \Delta\delta^2_{15N})^{1/2}]$ in chemical shift (hertz) of a backbone amide cross-peak as monitored by 2D {^{1}H,^{15}N}-HSQC NMR spectroscopy; $\Delta\delta_{total}$, the $\Sigma\Delta\delta_i$ over all monitored residues at each point of the titration; K_{D1}, dissociation constant of the first Ca^{2+} binding (to site II); K_{D2}, dissociation constant of the second Ca^{2+} binding (to site I); K_D, dissociation constant of $sTnI_{115-131}$ binding to sNTnC or $cTnI_{147-163}$ binding to cNTnC.

10.1021/bi001240u CCC: $19.00
Published on Web 09/16/2000

changes (*8*). This is mainly due to the fact that the regulatory domain of sTnC contains two functional Ca^{2+}-binding sites (sites I and II), while the same domain of cTnC contains only one active Ca^{2+}-binding site (site II). Site I in cNTnC is defunct on account of the lack of the first two Ca^{2+} coordinating ligands Asp^{29} and Asp^{31} and a Val^{28} insertion (for a review, see ref *9*). We have previously engineered an E41A mutant of sNTnC, in which the bidentate Ca^{2+} ligand Glu^{41} in site I is replaced by a nonliganding residue Ala (*10*). Like cNTnC, the structure of E41A-sNTnC also remains "closed" upon Ca^{2+} binding (*11*). Both E41A-sNTnC and cNTnC are modified in site I, albeit differently, suggesting a critical role for this region in the direct linkage between Ca^{2+} binding and the opening of the regulatory domain.

Ca^{2+} binding to TnC modifies the interaction of TnC and the inhibitory protein TnI, which plays a critical role in transmitting the Ca^{2+} signal to other proteins in the thin filaments (see reviews listed above). The exposed hydrophobic surface in the Ca^{2+}-saturated sNTnC has long been proposed as the sTnI binding site (*12*) and has subsequently been proven (*13*−*15*). The significant reduction in the exposure of the hydrophobic surface in Ca^{2+}-saturated cNTnC compared to Ca^{2+}-saturated sNTnC implies that the mode of interaction between cardiac TnC and TnI may be different than that between skeletal TnC and TnI. However, we have found that both cNTnC and sNTnC adopt similar conformations in binding their respective TnI regions (*14*, *16*, *17*). Specifically, $sTnI_{115-131}$ was found to bind to the hydrophobic core of Ca^{2+}-saturated sNTnC (*14*), and the corresponding $cTnI_{147-163}$ also interacts with the hydrophobic core of Ca^{2+}-saturated cNTnC and stabilizes the opening conformation of cNTnC (*17*). This region of TnI has been identified by many biological and biophysical studies to be the region responsible for binding to the regulatory domain of TnC, and this interaction modulates the interaction between the inhibitory regions of TnI and TnC (for reviews, see refs *18* and *19*). Thus, the pathway involved in initiating skeletal and cardiac muscle contraction is actually very similar. However, the kinetics and thermodynamics of the pathway must differ for the two systems to account for the different physiological behavior of the two muscle types.

To understand the unique delicate energetic balance that exists for each system, it is important to study the mechanism and energetics of the coupling between Ca^{2+}/TnI binding and induced structural changes in these important regulatory domains. Ca^{2+} and peptide titrations of the domain followed in detail by 2D $\{^1H,^{15}N\}$-HSQC NMR spectroscopy have been proven to be a powerful way of providing information such as binding stoichiometry, binding affinity, and binding kinetics. Using this technique, we have previously characterized the binding of Ca^{2+} and $sTnI_{115-131}$ to sNTnC (*14*, *20*), Ca^{2+} and $cTnI_{147-163}$ to cNTnC (*10*, *17*), and Ca^{2+} to E41A-sNTnC (*10*). In the present work, we have used the same method to investigate the binding of $sTnI_{115-131}$ peptide to E41A-sNTnC in the presence and absence of Ca^{2+}, respectively. We have also titrated E41A-sNTnC with Ca^{2+} in the presence of $sTnI_{115-131}$. In addition to obtaining the stoichiometry and affinity, the current work allows us to view the intimate coupling of Ca^{2+} and $sTnI_{115-131}$ binding to E41A-sNTnC. With this work, we have completed a series of ligand-binding studies on sNTnC, cNTnC, and E41A-sNTnC. Comparison of these binding properties allows us to dissect the mechanism of coupling of troponin structural opening and ligand binding intricately involved in the regulation of skeletal and cardiac muscle contraction. In turn, it allows us to understand further the differences between cardiac and skeletal muscle contraction.

EXPERIMENTAL PROCEDURES

Proteins and Peptides. The cloning, expression, purification, and decalcification of [^{15}N]-E41A-sNTnC were performed as described previously (*10*). The protein used for the titration of Ca^{2+}-saturated E41A-sNTnC with $sTnI_{115-131}$ was subjected to an additional step of reverse-phase HPLC purification on a SynChropak semipreparative C-8 column (250 mm × 10 mm, 300 Å pore size) with an adapted precolumn filter (0.2 μm). Both HPLC A and B buffers contained 200 mM ammonium acetate and 10 mM EDTA dissolved in HPLC grade H_2O (A buffer) or 50:50 water/acetonitrile (B buffer) at pH 6.5 and were filtered/degassed prior to use (0.2 μm pore size via vacuum filtration). The A to B elution gradient profile consisted of 12.5 min at 4% A to B per minute (i.e., gradient changed from 0 to 50% B) and then a slower gradient of 1% B per minute for 50 min during the protein elution. Collected protein was concentrated by freeze-drying, and metals were removed in the presence of EDTA on a G25 size exclusion column with ammonium bicarbonate buffer. The apo protein was repeatedly freeze-dried until no further change to the pH was detected. The synthetic $sTnI_{115-131}$ peptide, acetyl-RMSADAMLKALLG-SKHK-amide, was prepared as described previously (*13*). The peptide was lyophilized twice to remove residual organic solvent. Amino acid analysis, mass spectrometry, and analytical HPLC (at pH 2 using standard TFA/acetonitrile methodology) were used to establish the composition, concentration, mass, and purity of both the protein and the peptide.

NMR Samples. All NMR sample volumes were 500 μL (90% H_2O and 10% D_2O), consisting of 100 mM KCl, 10 mM imidazole, 0.01% NaN_3, and 0.1 mM 2,2-dimethyl-2-silapentane-5-sulfonate (DSS, as internal standard). The reported pH was not corrected for isotope effects, and the temperature of all NMR experiments was 30 °C.

Titration of Ca^{2+}-Saturated E41A-sNTnC with $sTnI_{115-131}$. To a NMR sample containing 1.5 mM [^{15}N]-E41A-sNTnC and 6 mM $CaCl_2$, aliquots of 5 μL of a first stock solution of $sTnI_{115-131}$ (3 mg of peptide dissolved in 55 μL of the NMR buffer) were added for the first 11 titration points and aliquots of 25 μL of a second stock solution (75 μL at approximately the same concentration as the first one) of $sTnI_{115-131}$ were added for the final 3 titration points. After spectra were acquired for each titration point, 5 μL of the NMR sample was set aside, and from this isolated portion of the sample, three separate 1 μL portions were used for amino acid analysis, which gives the $[sTnI_{115-131}]_{total}/[E41A\text{-}sNTnC]_{total}$ ratios of 0, 0.12, 0.19, 0.27, 0.44, 0.50, 0.62, 0.55, 0.70, 0.77, 0.94, 1.38, 1.70, 2.13, and 2.50, respectively. This technique resulted in a zero volume change for the titration, and the change in concentration of the protein and peptide was accommodated for in the dissociation constant calculations. Both the 1D ^1H and 2D $\{^1H,^{15}N\}$-HSQC NMR spectra were acquired at every titration point. The pH of the sample throughout the titration was approximately 6.70, and no pH adjustment was performed.

Titration of Apo E41A-sNTnC with $sTnI_{115-131}$. To a NMR sample containing 1.5 mM [^{15}N]-E41A-sNTnC, aliquots of 3 μL of a stock solution of $sTnI_{115-131}$ (5 mg of peptide dissolved in 50 μL of the NMR buffer) were added for the first 6 titration points and aliquots of 9 and 13 μL were added for the 7th and 8th points. A total of 1.23 mg of solid $sTnI_{115-131}$ peptide was added for the final titration point. The concentrations of E41A-sNTnC and peptide were determined by amino acid analysis, giving the $[sTnI_{115-131}]_{total}$/$[E41A\text{-}sNTnC]_{total}$ ratios of 0, 0.14, 0.28, 0.43, 0.57, 0.71, 0.86, 1.28, 1.90, and 2.56, respectively. Both the 1D ^{1}H and 2D {^{1}H,^{15}N}-HSQC NMR spectra were acquired at every titration point. The pH of the sample throughout the titration was approximately 6.70, and no pH adjustment was performed. Further addition of the $sTnI_{115-131}$ peptide to the apo E41A-sNTnC protein past a ratio of 3:1 resulted in the formation of a precipitate.

Titration of Apo E41A-sNTnC with Ca^{2+} in the Presence of $sTnI_{115-131}$. To a NMR sample containing 0.98 mM [^{15}N]-E41A-sNTnC and 2.8 mM $sTnI_{115-131}$, aliquots of 1 μL of 108 mM $CaCl_2$ were added for the first 8 points, 2 μL for the 9th, and 5 μL for the 10th point. The final molar equivalents of calcium to protein were 0, 0.22, 0.44, 0.66, 0.88, 1.09, 1.31, 1.53, 1.75, 2.18, and 3.31, respectively. Both the 1D ^{1}H and 2D {^{1}H,^{15}N}-HSQC NMR spectra were acquired at every titration point. The pH of the sample throughout the titration was approximately 6.70, and no pH adjustment was performed.

NMR Spectroscopy. All of the NMR spectra were obtained using Unity INOVA 500 MHz or Unity 600 MHz spectrometers at 30 °C. The 2D {^{1}H,^{15}N}-HSQC spectra were acquired using the sensitivity-enhanced gradient pulse scheme developed by Kay and co-workers (*21*, *22*). The ^{1}H and ^{15}N sweep widths were 7000 and 1600 Hz, respectively, on the 500 MHz spectrometer and were 8000 and 1650 Hz, respectively, on the 600 MHz spectrometer. All spectra were processed using NMRPipe (*23*), analyzed using PIPP (*24*), and referenced according to the IUPAC conventions. All directly and indirectly detected data sets were zero filled to twice the number of acquired points and apodized using a π/3 shifted sine bell before Fourier transformation.

RESULTS

Effects of $sTnI_{115-131}$ on E41A-sNTnC. The 2D {^{1}H,^{15}N}-HSQC NMR spectra of E41A-sNTnC in both the apo and Ca^{2+}-saturated states are completely assigned and used as starting points to monitor the $sTnI_{115-131}$-induced changes (*10*, *11*). Figure 1 shows the change in chemical shift of expanded regions of the 2D {^{1}H,^{15}N}-HSQC spectra of E41A-sNTnC·2Ca^{2+} upon addition of the $sTnI_{115-131}$ peptide. Cross-peaks corresponding to residues Ala^8, Phe^{22}, Phe^{26}, Asp^{27}, Ile^{37}, Thr^{39}, Met^{46}, Met^{48}, Asp^{59}, Ala^{60}, Val^{65}, Gln^{85}, and Met^{86} were observed to experience significant shifts in Figure 1A. Many of those residues are hydrophobic and buried in the closed structure of E41A-sNTnC·2Ca^{2+}. Thus it is likely that E41A-sNTnC·2Ca^{2+} opens to bind $sTnI_{115-131}$ in the otherwise blocked hydrophobic pocket. Most of the chemical shift changes fall into the fast exchange limit on the NMR time scale. The vast majority of the cross-peaks move in a linear fashion, but the residues involved in calcium

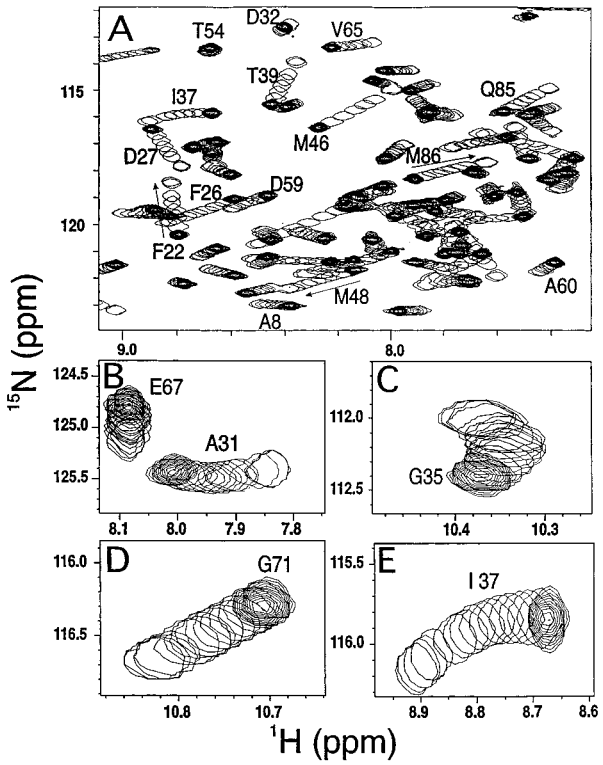

FIGURE 1: Contour plots of 2D {^{1}H,^{15}N}-HSQC NMR spectra from the backbone amide regions of E41A-sNTnC showing the effect of $sTnI_{115-131}$ addition to E41A-sNTnC·2Ca^{2+}. The E41A-sNTnC·2Ca^{2+} spectrum before the addition of peptide is shown with multiple contours while the spectra from each addition of $sTnI_{115-131}$ are indicated by single contours. The well-resolved residues are labeled with the single letter amino acid code, and the arrows indicate the direction of the change in chemical shift. An overall representative region is shown in panel A, and regions corresponding to several specific residues are shown in panels B−E.

binding site I (i.e., residues ~30−41) appear to move in a nonlinear, biphasic fashion. Figure 1B−E shows expanded plots of several residues displaying either linear (e.g., Glu^{67} and Gly^{71}) or nonlinear (e.g., Ala^{31}, Gly^{35}, and Ile^{37}) behavior upon peptide addition. The linear movement of some cross-peaks indicates that two protein species exist in the interaction between $sTnI_{115-131}$ and E41A-sNTnC·2Ca^{2+}. The position of each cross-peak corresponds to the weighted average of peptide free and bound E41A-sNTnC·2Ca^{2+}. This phenomenon was also observed in our earlier studies on $sTnI_{115-131}$ and $sTnI_{96-148}$ binding to sNTnC·2Ca^{2+} (*14*, *16*) and $cTnI_{147-163}$ binding to cNTnC·Ca^{2+} (*17*). Nonlinear movement of a cross-peak often indicates multiple binding of ligand to protein so that the position of a peak corresponds to the weighted average of a population of free and different bound species. However, in this case, only residues located in Ca^{2+}-binding site I (e.g., Ala^{31} and Gly^{35}) and the β-sheet (e.g., Ile^{73} and Asp^{74}) between site I and site II move in a nonlinear fashion. This indicates that these residues populate multiple conformational states in the Ca^{2+} and $sTnI_{115-131}$ binding equilibria as shown in Scheme 1. Since site I is the mutated site and is not fully Ca^{2+}-saturated, residues in this region may experience local $sTnI_{115-131}$-induced conformational rearrangement resulting in a more optimum coordinating environment in site I for Ca^{2+} (see below). On the other hand, residues located in site II show linear movement in chemical shift changes. This is likely due to its higher affinity

Scheme 1

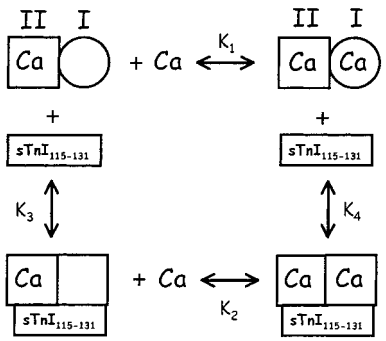

for Ca^{2+} and ability to remain fully saturated during the $sTnI_{115-131}$ titration.

In Scheme 1, site II is taken as fully Ca^{2+}-saturated, whereas site I populates multiple conformational states wherein the circle and square are as specified in the legend of Figure 4. K_1 and K_2 represent the dissociation constants of Ca^{2+} binding to site I in the absence and presence of $sTnI_{115-131}$, respectively; K_3 represents the dissociation constant of $sTnI_{115-131}$ binding to E41A-sNTnC with site I empty, and K_4 represents the dissociation constant of $sTnI_{115-131}$ binding to E41A-sNTnC with site I occupied by Ca^{2+}. Since the four equilibria constitute a closed scheme, the dissociation constants are related through the equation $K_1K_4 = K_3K_2$. From $K_1 = 2.49 \pm 0.36$ mM, $K_2 = 0.53 \pm 0.15$ mM, and $K_4 = 0.30 \pm 0.10$ mM (see below), K_3 is calculated to be 1.41 mM.

Residues that undergo backbone amide ^1H or ^{15}N chemical shift changes during titration can be followed to monitor $sTnI_{115-131}$ binding to the protein. The observed $\Delta\delta_{total}$ for all residues except those that undergo nonlinear movement was utilized to determine the dissociation constant of $sTnI_{115-131}$ binding to E41A-sNTnC·$2Ca^{2+}$. The average curve for all monitored amides is shown in Figure 1S (Supporting Information). The average change in chemical shift as a function of $[sTnI_{115-131}]_{total}/[E41A\text{-}sNTnC\cdot 2Ca^{2+}]_{total}$ for those amides was fit to the equation

$$E41A\text{-}sNTnC\cdot 2Ca^{2+} + sTnI_{115-131} \leftrightarrow E41A\text{-}sNTnC\cdot 2Ca^{2+}\cdot sTnI_{115-131} \quad (1)$$

and yielded a macroscopic dissociation constant (K_D) of 300 $\pm$ 100 μM. This is more than 10 times weaker than $sTnI_{115-131}$ binding to sNTnC·$2Ca^{2+}$ (*14*).

When $sTnI_{115-131}$ is titrated into apo E41A-sNTnC, most of the residues experience very minor chemical shift changes (Supporting Information, Figure 2S). Those changes were accompanied by some line broadening. This is most likely due to nonspecific interactions between the protein and the peptide. It is also possible that the atoms located on the exterior surface of E41A-sNTnC were affected by the presence of $sTnI_{115-131}$ in solution.

Effects of Ca^{2+} on E41A-sNTnC in the Presence of $sTnI_{115-131}$. Previously, we have performed the Ca^{2+} titration of E41A-sNTnC (*10*). Here we show the result from Ca^{2+} titration of E41A-sNTnC in the presence of $sTnI_{115-131}$ (Figure 2). The complete assignments for E41A-sNTnC in the apo and Ca^{2+}-saturated states (*10*, *11*) were used as a guide to monitor the Ca^{2+}-induced chemical shift changes

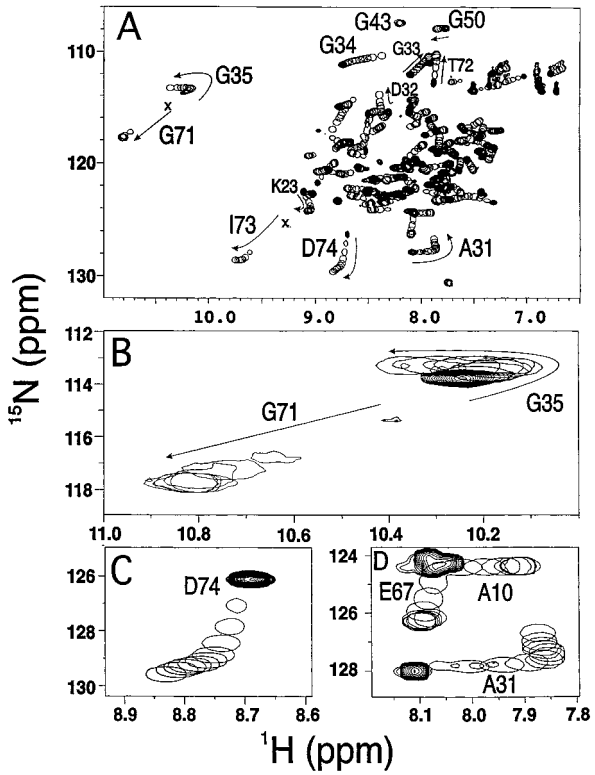

FIGURE 2: Contour plots of 2D {^1H,^{15}N}-HSQC NMR spectra of apo E41A-sNTnC in the presence of $sTnI_{115-131}$ showing the effect of calcium addition. The apo E41A-sNTnC spectrum before the addition of Ca^{2+} is shown with multiple contours while each addition of calcium is indicated by a single contour. The well-resolved residues are labeled with the single letter amino acid code, and the arrows indicate the direction of the change in chemical shift. The x indicates the starting positions of cross-peaks below the observable threshold. An overall representative region is shown in panel A, and regions corresponding to several specific residues are shown in panels B−D.

on the protein. Although a majority of the chemical shift changes fall into the fast exchange limit on the NMR time scale, some residues (e.g., Gly^{71} and Ile^{73}) are on intermediate/slow scale due to the relatively large chemical shift changes. The striking nonlinear, bidirectional movement of a number of residues, such as Gly^{35}, Ala^{31}, Ile^{73}, and Asp^{74}, clearly indicates the stepwise binding of Ca^{2+} to E41A-sNTnC in the presence of $sTnI_{115-131}$, i.e., site II followed by site I. This observation indicates that the order of Ca^{2+} binding to E41A-sNTnC is not altered by the presence of $sTnI_{115-131}$. To assess the effect of $sTnI_{115-131}$ on the Ca^{2+}-binding affinity, the chemical shift changes of Gly^{35} from this work were plotted as a function of $[Ca^{2+}]_{total}/[E41A\text{-}sNTnC]_{total}$ and compared with the Ca^{2+}-binding curve of the same residue from Ca^{2+} titration of E41A-sNTnC in the absence of $sTnI_{115-131}$ (Figure 3). Both binding curves were fitted individually to the equation

$$E41A\text{-}sNTnC + Ca^{2+} \leftrightarrow E41A\text{-}sNTnC\cdot Ca^{2+} + Ca^{2+} \leftrightarrow E41A\text{-}sNTnC\cdot 2Ca^{2+} \quad (2)$$

with K_{D1} and K_{D2} as the macroscopic dissociation constants for the binding of the first (i.e., to site II) and second (i.e., to site I) Ca^{2+} ions. For the titration in the absence of $sTnI_{115-131}$, the fitting yielded a K_{D1} of 24 $\pm$ 16 μM and a K_{D2} of 2.49 $\pm$ 0.36 mM, while for the titration in the presence

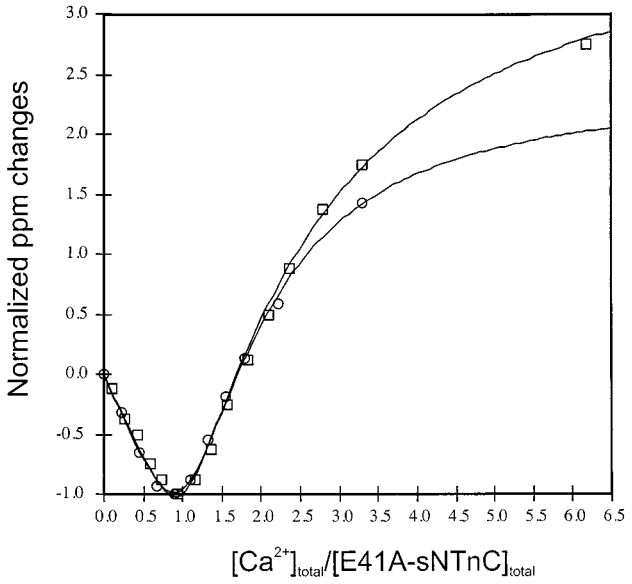

FIGURE 3: Ca^{2+}-binding curves of Gly^{35} from the 2D {^1H,^{15}N}-HSQC NMR spectral changes of apo E41A-sNTnC in the absence (□) and presence (○) of $sTnI_{115-131}$, respectively. The chemical shift changes were normalized to −1 when the $[Ca^{2+}]_{total}/[E41A\text{-}sNTnC]_{total}$ ratio is 1. The solid lines show the best-fitted curves. The fitted results are shown in Results.

of $sTnI_{115-131}$, the fitting yielded a K_{D1} of 14 ± 6 μM and a K_{D2} of 0.53 ± 0.15 mM. Direct comparison of the binding constants shows that the Ca^{2+} affinity of site II is altered slightly by the presence of $sTnI_{115-131}$ but that of site I is significantly increased (~5-fold). These results quantitatively support our conclusion (see above and Scheme 1) that the interaction of $sTnI_{115-131}$ and E41A-sNTnC induces a local conformational change in Ca^{2+}-binding site I to optimize the Ca^{2+} coordination sphere and, in turn, to increase its affinity for Ca^{2+}. As illustrated in Scheme 1, values of $K_1 = 2.49$ mM, $K_2 = 0.53$ mM, $K_3 = 1.41$ mM, and $K_4 = 0.3$ mM fit the experimental data corresponding to a Ca^{2+} affinity of site I increased by ~5-fold by the presence of $sTnI_{115-131}$ and, equally, a $sTnI_{115-131}$ binding affinity increased by ~5-fold by the presence of Ca^{2+} in site I.

Comparison of the Ca^{2+} and TnI Peptide Induced Chemical Shift Changes in sNTnC, E41A-sNTnC, and cNTnC. Figure 3S (Supporting Information) compares the plots of $\Delta\delta_{total}$ along the sequence for sNTnC, cNTnC, and E41A-sNTnC between the apo and Ca^{2+}-saturated states (Figure 3S, panels A−C, respectively) and between the Ca^{2+}-saturated and TnI peptide bound states (Figure 3S, panels D−F, respectively). The average values of $\Delta\delta_{total}$ are summarized in Table 1. The most immediate observation from Figure 3S and Table 1 is that the greatest magnitude of Ca^{2+}-induced chemical shift changes occurs for sNTnC. If the average $\Delta\delta_{total}$ for sNTnC is normalized to 100%, the $\Delta\delta_{total}$ amounts to 63% for cNTnC and 47% for E41A sNTnC (Table 1). The magnitude of chemical shift changes appears to be proportional to the degree of structural changes. The degree of structural opening can be quantified by the A/B and C/D interhelical angle changes from the apo to Ca^{2+}-bound state, and those changes are the biggest for sNTnC (~50° and ~70°, respectively), modest for cNTnC (~0° and ~10°, respectively), and the smallest for E41A sNTnC (~0° and ~0°, respectively) (*25*). Comparison of the peptide-induced $\Delta\delta_{total}$ reveals that sNTnC·$2Ca^{2+}$ experienced the

Table 1: Change in 2D {^1H,^{15}N}-HSQC Backbone Amide Cross-Peak Chemical Shifts for E41A-sNTnC, cNTnC, and sNTnC upon Addition of Ca^{2+} or TnI Peptide

protein/complex (condition)	average $\Delta\delta_{total}$ (Hz) (normalized value (%))
E41A-sNTnC (apo to Ca^{2+})[a]	98 (47)
cNTnC (apo to Ca^{2+})[a]	132 (63)
sNTnC (apo to Ca^{2+})[b]	209 (100)
E41A-sNTnC (Ca^{2+} to $sTnI_{115-131}$)[c]	75 (214)
cNTnC (Ca^{2+} to $cTnI_{147-163}$)[d]	84 (240)
sNTnC (Ca^{2+} to $sTnI_{115-131}$)[e]	35 (100)

[a] Data taken from ref *10*. [b] Data taken from ref *20*. [c] Data taken from this work. [d] Data taken from ref *17*. [e] Data taken from ref *14*.

smallest changes among the three. This is consistent with our earlier structural and binding studies of $sTnI_{115-131}$ (*14*) and $sTnI_{96-148}$ (*16*) which showed that these peptides bind to the open hydrophobic pocket of sNTnC·$2Ca^{2+}$ with minimal conformational perturbation. If the average $\Delta\delta_{total}$ for sNTnC·$2Ca^{2+}$ is normalized to 100%, the $\Delta\delta_{total}$ amounts to 240% for cNTnC·Ca^{2+} and 214% for E41A-sNTnC·$2Ca^{2+}$ (Table 1). When compared to sNTnC·$2Ca^{2+}$, cNTnC·Ca^{2+} experiences more than twice the amount of peptide-induced chemical shift changes as a result of a structural opening (A/B and C/D interhelical angle changes from cNTnC·Ca^{2+} to cNTnC·Ca^{2+}·$cTnI_{147-163}$ are ~30° and ~20°, respectively) (*17*). Although E41A-sNTnC·$2Ca^{2+}$ also experiences approximately twice the increase in $\Delta\delta_{total}$ than sNTnC·$2Ca^{2+}$, it is less than that observed for cNTnC·Ca^{2+}. It is interesting to note that the two hinge regions (*11*, *17*) (primarily on Glu^{40} or Glu^{41} and Val^{64} or Val^{65}) undergo a much larger peptide-induced change in cNTnC·Ca^{2+} than in E41A-sNTnC·$2Ca^{2+}$. In fact, Figure 1A shows that Val^{65} (^{15}N, ~113 ppm; ^1H, ~8.2 ppm, respectively, at the end of titration) did not move to the characteristic position (^{15}N, ~109 ppm; ^1H, ~7.3 ppm, respectively) for a fully "open" structure as observed in the case of sNTnC·$2Ca^{2+}$ (*26*) and cNTnC·Ca^{2+}·$cTnI_{147-163}$ (*17*). We know that cNTnC·Ca^{2+} upon binding $cTnI_{147-163}$ goes from an essentially closed state to a fully open state, similar to sNTnC·$2Ca^{2+}$. Thus, it is possible that E41A-sNTnC·$2Ca^{2+}$ experiences some degree of peptide-induced opening but the structure is not as fully open as sNTnC·$2Ca^{2+}$. This is likely due to the fact that although both cNTnC and E41A-sNTnC contain a modified Ca^{2+}-binding site I from sNTnC, this site is natural in cNTnC but damaged in E41A-sNTnC. Thus, the E41A-sNTnC·$2Ca^{2+}$·$sTnI_{115-131}$ complex may not be as stable as either sNTnC·$2Ca^{2+}$·$sTnI_{115-131}$ or cNTnC·$2Ca^{2+}$·$cTnI_{147-163}$. These results agree with our previous conclusion that, without the key residue Glu^{41}, the direct linkage between Ca^{2+} binding and the induced structural changes for sNTnC was broken (*11*). In turn, the interaction between sNTnC and $sTnI_{115-131}$ is perturbed, underscoring the critical role of this residue in skeletal muscle contraction.

DISCUSSION

This work is directed toward an understanding of the mechanism and energetics of coupling between Ca^{2+}/TnI peptide binding and the induced structural changes in the regulatory domain of TnC. In previous studies, we have performed detailed Ca^{2+} titrations of sNTnC, cNTnC, and E41A-sNTnC by monitoring changes in 2D {^1H,^{15}N}-HMQC

Table 2: Ca^{2+} and TnI Peptide Binding Parameters for sNTnC, cNTnC, and E41A-sNTnC[a]

	sNTnC	cNTnC	E41A-sNTnC	E41A-sNTnC (with $sTnI_{115-131}$)
$\Delta G°_1$ (kcal/mol)	−8.1[b]	−7.7[d]	−6.7[d]	−7.0[f]
$\Delta G°_2$ (kcal/mol)	−6.9[b]		−4.1[d]	−5.1[f]
$\Delta G°$ (kcal/mol)	−6.4[c]	−5.3[e]	−5.0[f]	

[a] The free energy was calculated from the standard relationship $\Delta G° = RT \ln K_D$. $\Delta G°_1$ represents the free energy for Ca^{2+} binding to site II, $\Delta G°_2$ represents the free energy for Ca^{2+} binding to site I, and $\Delta G°$ represents the free energy for $sTnI_{115-131}$ or $cTnI_{147-163}$ peptide binding. [b] Data taken from ref *20*. [c] Data taken from ref *14*. [d] Data taken from ref *10*. [e] Data taken from ref *17*. [f] Data taken from this work.

and {^{1}H,^{15}N}-HSQC NMR spectroscopy (*10*, *20*). We have also examined the binding of $sTnI_{115-131}$ to sNTnC·2Ca^{2+} (*14*), $sTnI_{96-148}$ to sNTnC·2Ca^{2+} (*16*), and $cTnI_{147-163}$ to cNTnC·Ca^{2+} (*17*). The present work focuses on the interaction of $sTnI_{115-131}$ and E41A-sNTnC and Ca^{2+} binding to E41A-sNTnC in the presence of $sTnI_{115-131}$. These results have allowed us to determine the stoichiometry and affinity of target binding to the regulatory domain of TnC and to assess the stability of the complexes involved.

The overall energetics of Ca^{2+} and TnI peptide binding to cNTnC and sNTnC necessarily reflect a delicate balance of several opposing forces, such as the favorable interactions of Ca^{2+}, peptide, and the protein and the unfavorable structural opening and resultant exposure of hydrophobic residues (for a detailed analysis on this subject, see refs *27* and *28*). In the apo state, sNTnC, E41A-sNTnC, and cNTnC all prefer closed conformations likely as a result of both favorable electrostatic and hydrophobic intramolecular interactions (for a review, see ref *25*). To accomplish a closed to open structural transition, the favorable free energy generated from Ca^{2+} and/or peptide binding has to be sufficient to outweigh the unfavorable energy barrier. It is not an easy task to measure this energy barrier due to the difficulties in detecting the open state of protein in the absence of Ca^{2+} or TnI. However, the energy barrier for a F29W mutant of sNTnC has been estimated to be ∼2.0 kcal·mol^{-1} by a low-temperature, high-pressure study (*29*).

To compare the energetics of Ca^{2+} and TnI peptide binding and induced structural changes in sNTnC, cNTnC, and E41A-sNTnC, we have summarized the dissociation constants from our previous and current work with the calculated binding free energies in Table 2 and constructed a schematic energy diagram as shown in Figure 4. A major observation from these data is that the free energy generated by the binding of TnI peptides to the closed E41A-sNTnC·2Ca^{2+} ($\Delta G° = \sim5.0$ kcal·mol^{-1}) or cNTnC·Ca^{2+} ($\Delta G° = \sim5.3$ kcal·mol^{-1}) proteins is less than that for binding to the open sNTnC·2Ca^{2+} ($\Delta G° = \sim6.4$ kcal·mol^{-1}) protein. This is most likely because the former interactions have to overcome the energy cost (Δ in Figure 4) of opening the protein before the peptide can bind. The energy difference of about 1.1−1.4 kcal·mol^{-1} is a direct result of the energy needed to open the structure of the regulatory domain after site II is Ca^{2+}-saturated. A $\Delta\Delta G°$ of 1.1−1.4 kcal·mol^{-1} corresponds roughly to the energetic barrier estimated by Foguel et al. (*29*). Although Foguel et al. has concluded that their estimation ($\Delta G = \sim2.0$ kcal·mol^{-1}) reflects the conformational change that precedes Ca^{2+} binding to sNTnC (i.e., the opening of the apo protein), the fact that our measurement is of comparable magnitude suggests that they may have also observed the same conformational change. Since the F29W mutation resides in the center of the Ca^{2+}-binding site I, the fluorescence measurement by probing the tryptophan environment may provide only local conformational information.

In sNTnC, binding of a single Ca^{2+} to site II is favorable by −8.1 kcal·mol^{-1} (*10*, *20*) (Figure 4 and Table 2). This step is accompanied by relatively minor structural changes and sets the stage for Ca^{2+} binding to site I (*30*). Binding of a second equivalent of Ca^{2+} to site I in sNTnC provides −6.9 kcal·mol^{-1} of free energy. This step allows sNTnC to overcome the energy barrier ($\Delta G° = \sim1-2$ kcal·mol^{-1}) and adopts an open conformation. Subsequently, $sTnI_{115-131}$ binds to the exposed hydrophobic surface and provides an additional contribution of −6.4 kcal·mol^{-1} to the stability of the sNTnC·2Ca^{2+}·$sTnI_{115-131}$ complex (*14*). Thus, Ca^{2+} binding to site I is the main driving force for the opening of sNTnC, and the opening of the structure of sNTnC·2Ca^{2+} is energetically favorable (Figure 4).

Similarly, Ca^{2+} binding to site II of E41A-sNTnC provides −6.7 kcal·mol^{-1} of free energy, which sets the stage for Ca^{2+} binding to site I (Figure 4 and Table 2). However, the E41A mutation destabilizes Ca^{2+}-binding site I by 2.8 kcal·mol^{-1} (−6.9 to −4.1 kcal·mol^{-1}) (*10*). Since Ca^{2+} binding to site I accounts for the large conformational changes and the opening of the structure, this reduction in Ca^{2+}-binding free energy apparently sabotages the ability of E41A-sNTnC to overcome the energetic barrier ($\Delta G° = \sim1-2$ kcal·mol^{-1}). As a result, E41A-sNTnC·2Ca^{2+} remains in a closed conformation (*11*). The interaction of $sTnI_{115-131}$ with E41A-sNTnC·2Ca^{2+} provides a net $\Delta G°$ of −5.0 kcal·mol^{-1}. This corresponds to the free energy released from the formation of the E41A-sNTnC·2Ca^{2+}·$sTnI_{115-131}$ complex minus the energy needed to open the structure. Thus, $sTnI_{115-131}$ binding compensates the reduction of the driving force (Ca^{2+} binding to site I) for the opening of E41A-sNTnC.

In cNTnC, binding of a single Ca^{2+} to site II provides −7.7 kcal·mol^{-1} of free energy (*10*) (Figure 4 and Table 2). This binding is accompanied by little structural change, and cNTnC·Ca^{2+} remains closed (*8*). The defunct site I prohibits binding of a second equivalent of Ca^{2+}. The cardiac peptide $cTnI_{147-163}$ binds to cNTnC·Ca^{2+} with a $\Delta G°$ of −5.3 kcal·mol^{-1} (*17*). This is sufficient to overcome the energy barrier for the opening of cNTnC·Ca^{2+}. Thus, the binding of $cTnI_{147-163}$ to cNTnC contributes a major part to the structural opening in the cardiac pathway, unlike the skeletal pathway.

The free energy differences between Ca^{2+}/peptide binding to E41A-sNTnC·2Ca^{2+} and to sNTnC·2Ca^{2+} can be attributed to the mutation E41A. Glu^{41} is the important bidentate-coordinating ligand to Ca^{2+} in site I and serves as a direct linkage between Ca^{2+} binding and the resultant opening of the structure of sNTnC (*11*). The mutation of Glu^{41} to Ala^{41} introduces several possible energetic/stability effects. The loss of the $-CH_2-COO^-$ portion of Glu^{41} reduces the overall negative charge in a metal binding pocket and should stabilize the apo structure in addition to decreasing the metal affinity. The substitution of a charged residue for a hydrophobic one should also stabilize the hydrophobic core packing and favor a more closed structure. However, Ala^{41} has a higher helical propensity and should therefore

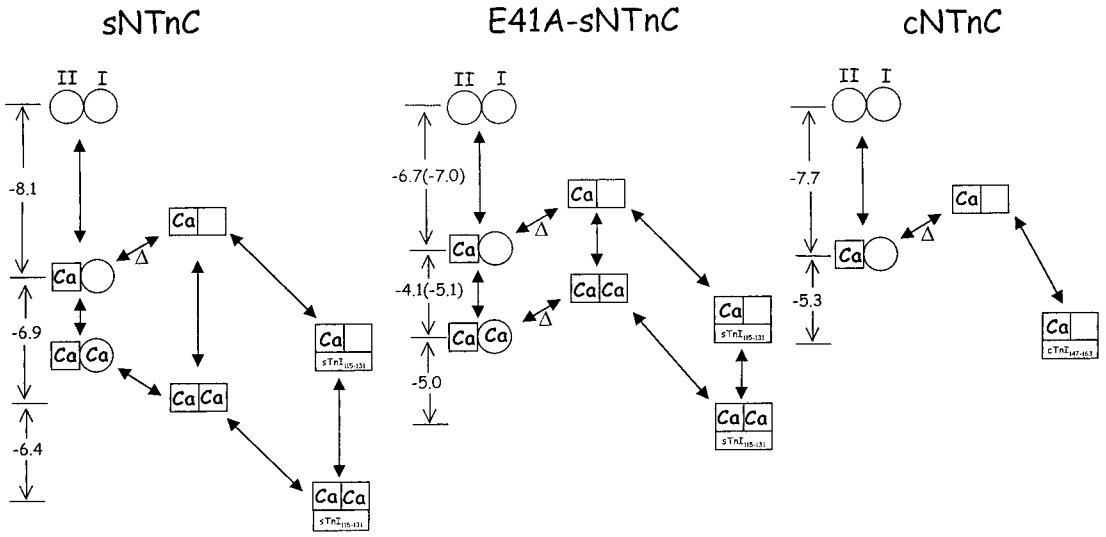

FIGURE 4: Schematic view of the relative free energies ($\Delta G°$ in kcal·mol^{-1}) of sNTnC, E41A-sNTnC, and cNTnC upon ligand binding. The free energies are from Table 2. The possible equilibria are marked by diamond-headed arrows. The circle represents a local structure indicative of the closed state for the Ca^{2+} binding site specified, while the square represents a local structure indicative of the open state for the Ca^{2+}-binding site specified. Thus, the two circles represent a closed conformation for the specified protein domain, a square for site II and a circle for site I indicate that site II adopts a conformation posed to be open and sets the stage for the opening of the domain, and two squares represent an open conformation for the specified protein domain. The energy levels of the apo states of the proteins are placed at arbitrary levels.

favor an extension of the B-helix and consequently the open conformation (*11*). The sum of these effects is reflected in the observed Ca^{2+}/TnI peptide-binding affinities and the conformations adopted by E41A-sNTnC in the free and bound states. The E41A mutation not only destabilizes Ca^{2+} binding to site I by 2.8 kcal·mol^{-1} but also destabilizes Ca^{2+} binding to site II by 1.4 kcal·mol^{-1} (from -8.1 to -6.7 kcal·mol^{-1}) due to the structural coupling between the two sites (see detailed discussions in refs *10* and *11*)). In addition, the present results show that this mutation disturbs the interaction of the protein and TnI peptide. On the basis of the chemical shift measurements, we have suggested that E41A-sNTnC adopts a less open structure in the E41A-sNTnC·2Ca^{2+}·sTnI$_{115-131}$ complex than sNTnC in the sNTnC·2Ca^{2+}·sTnI$_{115-131}$ complex. This conclusion is supported by a recent study on the E140Q mutant of the C-domain of calmodulin (*31*). In the work, the first Ca^{2+} binding induced minor structural changes, and the domain is essentially closed. The major structural changes were observed upon binding of the second Ca^{2+}. However, the E140Q mutation reduces the Ca^{2+}-binding affinity and prevents the protein from completely exposing the hydrophobic surface. As a result, the Ca^{2+} saturated form of the E140Q calmodulin C-domain experiences a global conformational equilibrium between 65% open and 35% closed states.

A second major issue that arises from this study is the observation that site I responds uniquely to the interaction between E41A-sNTnC·2Ca^{2+} and sTnI$_{115-131}$, demonstrating the intimate coupling of sTnI$_{115-131}$ and Ca^{2+} binding to site I (see Scheme 1). By thermodynamic arguments, if the protein interacts with another protein in a Ca^{2+}-dependent manner, the presence of that protein will also increase the Ca^{2+} affinity. This is exactly our observation in that the Ca^{2+}-binding affinity of site I is enhanced ~5-fold ($K_1/K_2 = 4.7$) by the presence of sTnI$_{115-131}$. To satisfy the thermodynamic equilibria cycle in Scheme 1, K_3/K_4 therefore must equal to K_1/K_2. Thus, the ratio of $K_3/K_4 = 4.7$ indicates that the sTnI$_{115-131}$-binding affinity is also enhanced ~5-fold by the presence of Ca^{2+} in site I. A similar phenomenon has been observed from the Ca^{2+}-binding studies of E140Q (site IV mutation) and E104Q (site III mutation) mutants of the calmodulin C-domain (*31*, *32*). These studies showed that when Ca^{2+} is present in the nonmutated site, the mutated site experiences multiple populated states. This unique behavior was not observed with wild-type sNTnC (*14*) or cNTnC (*17*). The present results provide a rare view into the molecular events behind the overall cooperative Ca^{2+} and TnI binding to sNTnC and cNTnC.

The ~5-fold affinity enhancement of sTnI$_{115-131}$ for E41A-sNTnC by the presence of Ca^{2+} in site I may be compared with previous studies (for a review, see ref *3*; see also refs *33* and *34*) on the coupling between Ca^{2+} and TnI binding to TnC. The cumulative data of these reports indicate that the effect of the presence of Ca^{2+} ions on the interaction of TnC and TnI inhibitory peptide leads to an increase in affinity of 6−10-fold over that seen under apo or plus Mg^{2+} conditions. However, this effect on the interaction of TnC and intact TnI is much greater, where the presence of Ca^{2+} increases affinity 40−120-fold over that seen under plus Mg^{2+} conditions and 1000−8000-fold compared with the apo state (*35*, *36*). From this perspective, the affinities of TnI peptides for TnC only partially reflect the influence of Ca^{2+} signal on the interaction of TnC and intact TnI. Clearly, other regions of the TnI molecule are of vital importance in conferring such a high degree of Ca^{2+} sensitivity to the interaction of these two proteins.

The above analysis shows that Ca^{2+} and TnI peptide binding to the regulatory domain of sTnC or cTnC and the accompanying conformational changes are governed by a delicate energetic balance for each system. The energy barrier of opening the closed protein is indeed quite low. The energy barrier of ~1−2 kcal·mol^{-1} would suggest that ~5−15% of the regulatory domain may be open at any given time

after site II is Ca^{2+}-saturated. The energetics of the coupling between Ca^{2+}/TnI peptide binding determined herein help us to understand that the differences between skeletal and cardiac muscle physiology are not a result of different structures but of a different balance of populations of the various conformational states involved.

ACKNOWLEDGMENT

We thank Gerry McQuaid for maintaining the spectrometers, Brian Tripet and Pascal Mercier for insightful discussions, Leo Spyracopoulos for ideas and feedback, and David C. Corson for expression and purification of the E41A-sNTnC protein.

SUPPORTING INFORMATION AVAILABLE

Figure 1S showing the binding curve of E41A-sNTnC·$2Ca^{2+}$ upon $sTnI_{115-131}$ addition, Figure 2S showing a contour plot of apo E41A-sNTnC and the effect of $sTnI_{115-131}$ addition, and Figure 3S showing chemical shift changes for backbone amide pairs in E41A-sNTnC, cNTnC, and sNTnC. This material is available free of charge via the Internet at http://pubs.acs.org.

REFERENCES

1. Finn, B. E., and Drakenberg, T. (1999) *Adv. Inorg. Chem. 46*, 441−494.
2. Gergely, J. (1998) *Adv. Exp. Med. Biol. 453*, 169−176.
3. Perry, S. V. (1999) *Mol. Cell. Biochem. 190*, 9−32.
4. Filatov, V. L., Katrukha, A. G., Bulargina, T. V., and Gusev, N. B. (1999) *Biochemistry (Moscow) 64*, 969−985.
5. Slupsky, C. M., and Sykes, B. D. (1995) *Biochemistry 34*, 15953−15964.
6. Sia, S. K., Li, M. X., Spyracopoulos, L., Gagné, S. M., Liu, W., Putkey, J. A., and Sykes, B. D. (1997) *J. Biol. Chem. 272*, 18216−18221.
7. Gagné, S. M., Tsuda, S., Li, M. X., Smillie, L. B., and Sykes, B. D. (1995) *Nat. Struct. Biol. 2*, 784−789.
8. Spyracopoulos, L., Li, M. X., Sia, S. K., Gagné, S. M., Chandra, M., Solaro, R. J., and Sykes, B. D. (1997) *Biochemistry 36*, 12138−12146.
9. Tobacman, L. S. (1996) *Annu. Rev. Physiol. 58*, 447−481.
10. Li, M. X., Gagné, S. M., Spyracopoulos, L., Kloks, C. P. A. M., Audette, G., Chandra, M., Solaro, R. J., Smillie, L. B., and Sykes, B. D. (1997) *Biochemistry 36*, 12519−12525.
11. Gagné, S. M., Li, M. X., and Sykes, B. D. (1997) *Biochemistry 36*, 4386-4392.
12. Herzberg, O., Moult, J., and James, M. N. G. (1986) *J. Biol. Chem. 261*, 2638−2644.
13. Tripet, B. P., Van Eyk, J. E., and Hodges, R. S. (1997) *J. Mol. Biol. 271*, 728−750.
14. McKay, R. T., Tripet, B. P., Hodges, R. S., and Sykes, B. D. (1997) *J. Biol. Chem. 272*, 28494−28500.
15. McKay, R. T., Tripet, B. P., Pearlstone, J. R., Smillie, L. B., and Sykes, B. D. (1999) *Biochemistry 38*, 5478−5489.
16. McKay, R. T., Pearlstone, J. R., Corson, D. C., Gagne, S. M., Smillie, L. B., and Sykes, B. D. (1998) *Biochemistry 37*, 12419−12430.
17. Li, M. X., Spyracopoulos, L., and Sykes, B. D. (1999) *Biochemistry 38*, 8289−8298.
18. Farah, C. S., and Reinach, F. C. (1995) *FASEB J. 9*, 755−767.
19. Solaro, R. J., and Rarick, H. M. (1998) *Circ. Res. 83*, 471−480.
20. Li, M. X., Gagné, S. M., Tsuda, S., Kay, C. M., Smillie, L. B., and Sykes, B. D. (1995) *Biochemistry 34*, 8330−8340.
21. Kay, L. E., Keifer, P., and Saarinen, T. (1992) *J. Am. Chem. Soc. 114*, 10663−10665.
22. Zhang, O., Kay, L. E., Olivier, J. P., and Forman-Kay, J. D. (1994) *J. Biomol. NMR 4*, 845−858.
23. Delaglio, F., Grzesiek, S., Vuister, G. W., Zhu, G., Pfeifer, J., and Bax, A. (1995) *J. Biomol. NMR 6*, 277−293.
24. Garrett, D. S., Powers, R., Gronenborn, A. M., and Clore, G. M. (1991) *J. Magn. Reson. 95*, 214−220.
25. Gagne, S. M., Li, M. X., McKay, R. T., and Sykes, B. D. (1998) *Biochem. Cell Biol. 76*, 302−312.
26. Gagné, S. M., Tsuda, S., Li, M. X., Chandra, M., Smillie, L. B., and Sykes, B. D. (1994) *Protein Sci. 3*, 1961−1974.
27. Nelson, M. R., and Chazin, W. J. (1998) *Biometals 11*, 297−318.
28. Nelson, M. R., and Chazin, W. J. (1998) *Protein Sci. 7*, 270−282.
29. Foguel, D., Suarez, M. C., Barbosa, C., Rodrigues, J. J., Jr., Sorenson, M. M., Smillie, L. B., and Silva, J. L. (1996) *Proc. Natl. Acad. Sci. U.S.A. 93*, 10642−10646.
30. Strynadka, N. C. J., Cherney, M., Sielecki, A. R., Li, M. X., Smillie, L. B., and James, M. N. G. (1997) *J. Mol. Biol. 273*, 238−255.
31. Evenas, J., Thulin, E., Malmendal, A., Forsén, S., and Carlstrom, G. (1997) *Biochemistry 36*, 3448−3457.
32. Evenas, J., Malmendal, A., Thulin, E., Carlstrom, G., and Forsen, S. (1998) *Biochemistry 37*, 13744−13754.
33. Swenson, C. A., and Fredricksen, R. S. (1992) *Biochemistry 31*, 3420−3429.
34. Pearlstone, J. R., and Smillie, L. B. (1995) *Biochemistry 34*, 6932−6940.
35. Ingraham, R. H., and Swenson, C. A. (1984) *J. Biol. Chem. 259*, 9544−9548.
36. Wang, C. K., and Cheung, H. C. (1985) *Biophys. J. 48*, 727−739.

BI001240U